ORIGINAL PAPER

Synthesis of Novel Carbazole Fused Coumarin Derivatives and DFT Approach to Study Their Photophysical Properties

Nagaiyan Sekar · Prashant G. Umape · Sandip K. Lanke

Abstract Novel coumarin derivatives have been synthesized by the classical Knoevenagel condensation of 4-hydroxy-9-methyl-9H-carbazole-3-carbaldehyde with active methylene compounds and characterized. Effect of solvent polarity on the photophysical properties, absorption and emission has been studied. The photophysical properties of the synthesized coumarins have been compared with some of the established analogous coumarin derivatives. Investigation of the structural parameters and understanding photophysical properties of the synthesized coumarin derivatives were carried out using Density Functional Theory (DFT) and Time Dependant Density Functional Theory (TDDFT) computations. The experimental values were correlated with the theoretical derived results. The ratio of the excited state and the ground state dipole moments was calculated by using solvatochromic and solvatofluoric data and compared with the values obtained from DFT and TDDFT computations.

N. Sekar (✉) · P. G. Umape · S. K. Lanke
Tinctorial Chemistry Group, Department of Dyestuff Technology, Institute of Chemical Technology, (Formerly UDCT), Nathalal Parekh Marg, Matunga, Mumbai 400 019, India
e-mail: n.sekar@ictmumbai.edu.in

N. Sekar
e-mail: nethi.sekar@gmail.com

Introduction

Fluorescent coumarins are known for high quantum yield, excellent light stability, large Stokes' shift and low toxicity [1]. They can be tailored easily depending upon the applications. Due to their excellent fluorescent properties, they have significant functional applications in industry and research. They are widely used as laser dyes [2], fluorescent whiteners [3], organic nonlinear optical material [4, 5], coumarin derivatives are extensively investigated as probes for biological applications, in particular for in vivo imaging of cells in living organisms [6–8].

A series of novel coumarin derivatives linked with an N,N-dimethylaniline group via cyclopentanonediene on position 4 of the coumarin ring were synthesized and their two-photon absorbing (TPA) properties were investigated [9]. Among the coumarin colorants 7-aminocoumarin derivatives are widely used as blue laser dyes as well as florescence probes in many chemical and physicochemical studies [10–13]. The fluorescence property of the coumarin chromophore system is significantly altered by changing the appropriate substituent's at the 3- and the 7-position. Coumarin scaffold with electron donor at 7-position and electron withdrawing groups at 3 positions impart enhanced fluorescence quantum yield, and bathochromicity [14, 15]. In the case of substituted 7-aminocoumarin derivatives free rotation of the substituted amino group influences the fluorescence properties by non-radiative decay, and hence rigidized 7-amino substitution enhances the intramolecular charge transfer leading to enhanced fluorescence properties [16–18].

In accordance with the above discussion, carbazole is electron rich planar molecule, which is isoelectronic with diphenylamine [19, 20]. They are well known as a conjugated, good hole transporting, electron-donor and planar compounds. It is of interest in terms of both optical and electronic applications such as photoconductivity, photo-refractivity and high charge mobility.

Carbazole derivatives have been used as fluorescent markers, charge transfer agents, solar energy collectors, and nonlinear optical two-photon absorbing materials [21–23]. Carbazole unit has an electron donating influence and carbazole containing dyes are known to have excellence photoconductivity and relatively intense luminescence [24]. The thermal stability or the glass state durability of the organic compounds can be greatly enhanced by the introduction of carbazole moiety in the core structure [25]. The N-alkyl carbazole compounds have shown excellent thermal and good electro-optical properties [26].

Hence, in order to address the above challenges, herein we prepared new coumarin fused carbazole derivatives and studied their photophysical properties.

Results and Discussion

The classical Knoevenagel condensation was carried out between 4-hydroxy-9-methyl-9*H*-carbazole-3-carbaldehyde **4** and the different active methylene compounds (**5a–5d**) to give the respective carbazole based coumarin derivatives **6a–6d**. Here, methylation of 4-hydoxy carbazole **1** gives 4-methoxy-9-methyl-9*H*-carbazole **2** and the subsequent Vilsmeier-Haack formylation of 4-methoxy-9-methyl-9*H*-carbazole **2** gives mixture of 4-methoxy-9-methyl-9*H*-carbazole-3-carbaldehyde **3** and 4-methoxy-9-methyl-9*H*-carbazole-1-carbaldehyde **3a**. The mixtures of aldehydes were separated by column chromatography and 4-methoxy-9-methyl-9*H*-carbazole-3-carbaldehyde **3** was subjected to demethylation using AlCl₃ as a catalyst [27]. The obtained 4-hydroxy-9-methyl-9*H*-carbazole-3-carbaldehyde **4** on Knoevenagel condensation with the different active methylene moieties such as malononitrile, 2-cyanomethyl-1,3-benzothiazole, 2,2-dimethyl-1,3-dioxane-4,6-dione (meldrum's acid) and p-nitrobenzyl cyanide gives respective carbazole based coumarin derivatives **6a–6d** (Scheme 1).

Photophysical Properties

The coumarin fluorophores **6a–6d** synthesized here are yellow to orange colored. They are having good blue colored fluorescence. Figure 1 represents photographs of the synthesized coumarin derivatives in daylight and UV light. These coumarin derivatives absorb in the range 381–417 nm. The coumarin **6d** has dual absorption in DMF at 417 and 602 nm. Figure 2a represents overlay absorption maxima of the synthesized coumarins **6a–6d** in ethanol. The coumarin derivatives **6a**, **6b** and **6c** absorb at close proximity and a blue shifted emission is observed in the case of the coumarin **6c** with carboxylic substitution at the 3rd position to the lactone ring. The emission maxima of the synthesized coumarin derivatives **6a–6c** lies in the range of 463–496 nm, while

coumarin **6d** has dual emission in chloroform, dichloromethane and DMF. Figure 2b is overlay emission spectra of the synthesized coumarin derivatives in ethanol showing excellent emissive properties of the coumarin derivatives **6b** and **6c** and the coumarin **6d** shows very weak emissive characteristics amongst the coumarin derivatives reported in this paper. Further the effects of solvent polarity on the absorption and emission properties of these molecules were studied and the ratio of excited state dipole moment to the ground state dipole moment was calculated by the solvatochromic method as well as DFT and TD-DFT computations.

Solvatochromism and Solvatofluorism

The fluorophores with the donor and acceptor terminals bridged by the olefinic conjugated systems involves intramolecular charge transfer phenomenon. Such fluorescent molecules are polarized and their photophysical properties are affected by the properties of the surrounding media. Hence, we have studied the effect of the solvent polarities on the photophysical properties of the synthesized dyes. Also, the synthesized novel coumarin derivatives **6a–6d** are subjected to analysis effect of solvent polarity on their absorption and emission characteristics. The data obtained are summarized in Tables S8.

The absorption characteristics of the coumarin derivative **6a** with a cyano-substitution at the 3 position are not affected dramatically by the polarity of the solvents, the absorption maxima is found to be in the range 398–407 nm. It absorbs with a maximum intensity in chloroform (Fig. 3). A similar characteristic is shown by the coumarin analogue **6b** whose absorption maxima range is 399–405 nm. The maximum absorbance is observed in acetone, while minimum in THF (Fig. 3). The coumarin **6c** shows bathochromic shift in absorption in non polar solvents. It absorbs at 381 nm in polar solvents while in chloroform and dichloromethane absorption is seen at 405 nm. Also, a strong absorbance is seen in dichloromethane and weaker one in THF (Fig. 3). The coumarin derivative **6d** shows dual absorption at 417 and 603 nm in DMF, while in all the other solvents the absorption ranges from 399 to 411 nm. It absorbs with strong intensity in chloroform while in DMF weak absorption intensity is observed (Fig. 3).

The synthesized coumarin derivatives have excellent fluorescent characteristics and it is due to the rigid structural arrangement. We studied the effect of polarity of solvent on emissive properties of these novel coumarin analogues and the emission data is summarized in (Table S8, Supporting Info). Figure 2b represents overlay emission spectra of the synthesized coumarin derivatives in different solvents of different polarities. The coumarin derivative **6a** shows bathochromic shift in emission maxima from 474 to 491 nm with an increase in the solvent polarity. In DMF, it has the longest emission

Scheme 1 Synthesis of coumarin derivatives **6a–6d**
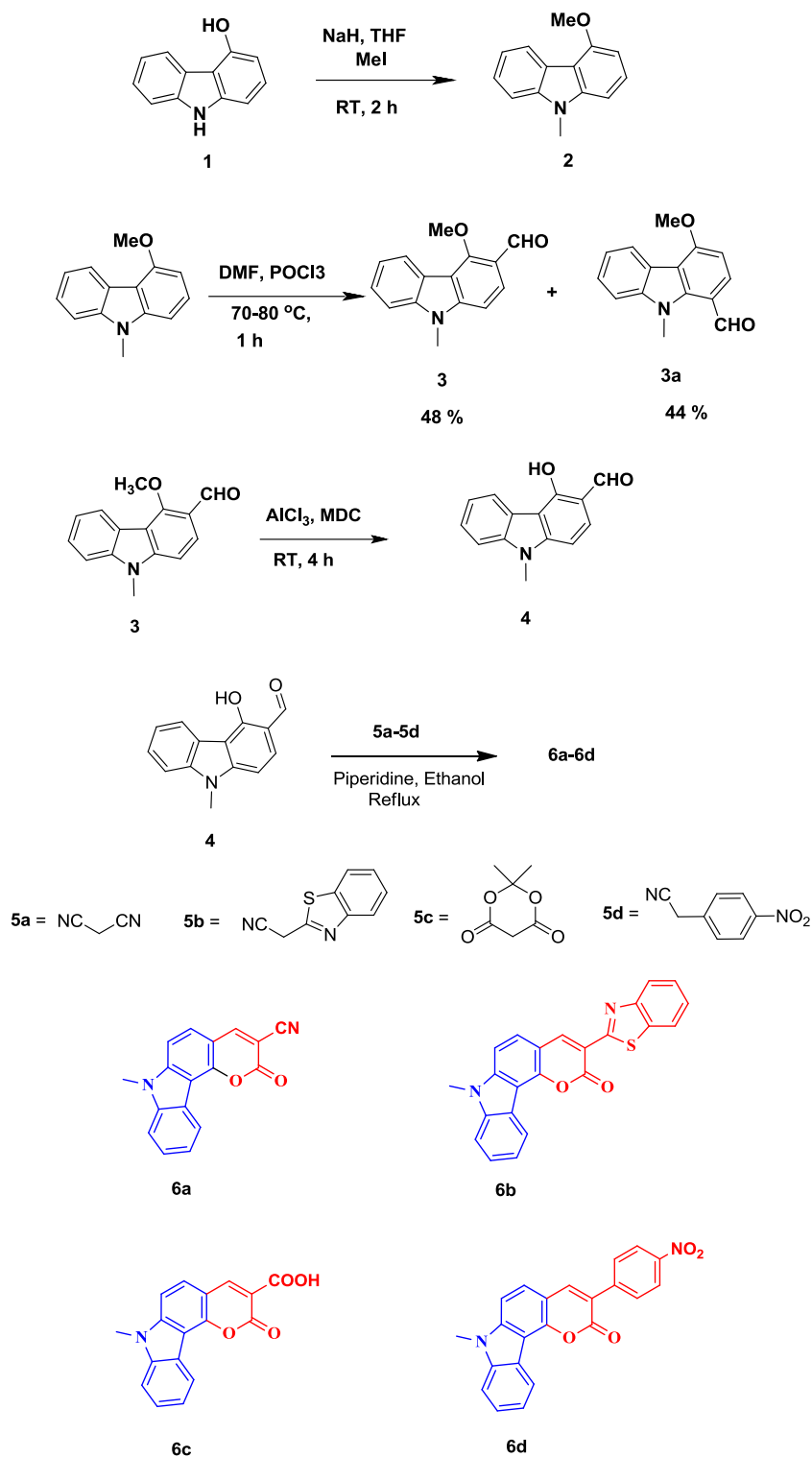
maxima and has appreciable emission intensity in ethyl acetate and THF (Fig. 4).

It is evident that the coumarin analogue **6b** shows bathochromically shifted emission maxima in the polar solvents. The largest red shift is observed in methanol at 496 nm while a blue shifted emission maximum is observed in ethyl acetate and THF at 468 and 467 nm respectively (Table S8). A strong emission is observed in acetonitrile, ethanol and methanol Fig. 4. The coumarin analogue **6c** emits in the range 466–486 nm. The emission properties of **6c** show bathochromic emission in acetone at 482 nm and in acetonitrile at 486 nm; however, hypsochromic emissions are observed in ethyl

Fig. 1 UV-light and day-light images of coumarin derivatives **6a–6d**
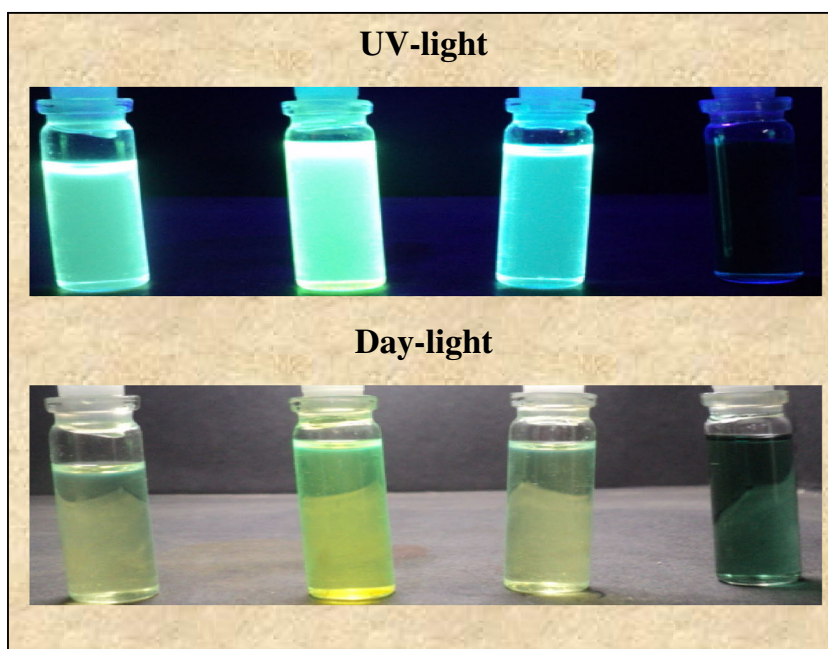
acetate, methanol, and DMF. Figure 4 represents overlay emission maxima of the fluorophore **6c** in different solvents of varying polarity. Fluorophore **6c** clearly indicates excellent emissive property in acetone, methanol, acetonitrile and ethanol. The coumarin derivative **6d** shows a peculiar property of dual emission in chloroform and dichloromethane. The observed emission shows the first peak at 485 nm and the second at 606 nm in chloroform, 479 and 566 nm in dichloromethane. It has blue emission between 481 and 495 nm in polar solvents such as methanol, acetonitrile and ethanol. It shows a remarkable bathochromic shift in non-polar solvents. The longest emission is observed in acetone at 613 nm, while in ethyl acetate and THF it emits at 564 and 566 nm respectively (Table 4). Excellent emission intensity is observed in THF and ethyl acetate. In DMF, the fluorescence is almost quenched Fig. 4.

The Stokes' shift values are reported in Tables S8 which shows that there is an elevation in Stokes' shift with increasing

solvent polarity for the coumarin analogue **6a**. The largest Stokes' shift of 95 nm is observed in polar protic solvents and lower value of 68 nm is observed in chloroform. In the case of the coumarin **6b** similar results are seen, the Stokes' shift increases with an increase in solvent polarity. In methanol the largest Stokes' shift of 94 nm is observed and the lowest value of Stokes' shift 65 nm is observed in chloroform. A clear increment is depicted in Stokes' shift by the coumarin **6c** with increasing solvent polarity. It emits with the largest Stokes' shift 105 nm in acetonitrile, and the shortest one 68 nm in chloroform. As coumarin analogue **6d** has distinctive photophysical properties in chloroform, dichloromethane and DMF, in these solvents two emissions are observed, hence it has two Stokes' shifts in each solvent. In chloroform, Stokes' shift of 74 and 195 nm are observed for the emission maxima of 485 and 606 nm. In dichloromethane, Stokes' shift of 68 and 197 nm are observed corresponding to the emission at 479 and 608 nm. In DMF, dual absorption as well as

Fig. 2 **a** Overlay absorption spectra of coumarins **6a–6d** in ethanol, **b** Overlay emission spectra of coumarins **6a–6d** in ethanol
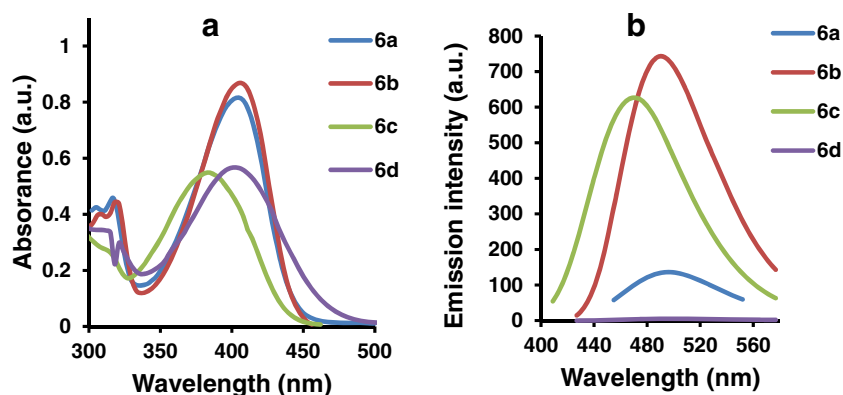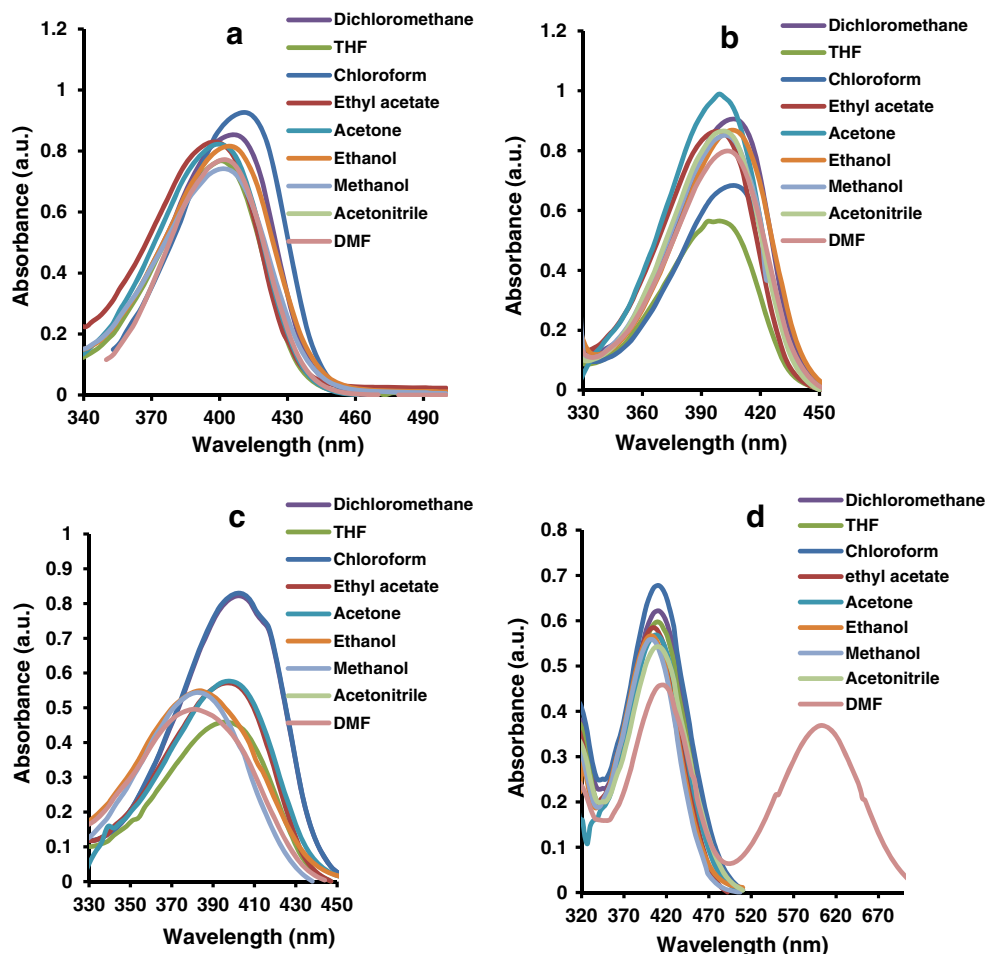
Fig. 3 Absorption spectra of dye 6a–6d in different solvents

emissions are observed and the corresponding Stokes' shifts are 86 and 72 nm. In the remaining non polar solvents such as acetone, THF quite impressive large Stokes' shifts ranging from 205 nm in acetone to 155 nm in THF are observed. From Table S8, the fluorescence excitation maxima of the coumarin analogue 6a have nearly same values. The coumarin derivatives 6b and 6c shows excitation maxima at longer wavelength than the absorption maxima (Fig. 3). In the case of the coumarin 6d for two emission two different excitation maxima are recorded. These excitation maxima are more red shifted than the absorption maxima except in methanol, and DMF, excitation maxima corresponding to the emission at 481 nm, in methanol and 503 nm in DMF have hypsochromic shift than the respective absorption maxima.

The spectral properties of the model dye 6b were compared with established dyes 7–9. The comparative data are summarized in Table 1. It is clearly evident that the dye 6b displayed a remarkable hypsochromic shift in absorption and emission properties and a comparatively larger Stokes' shift relative to the established dyes 7 and 9, while it is matching with dye 8. This is because of two nitrogen donor group are present at 6, 7 position of coumarin scaffold as compared to dye 6b.

Dipole Moment Determination by Solvatochromic Method

These synthesized coumarin analogues show remarkable effect of solvent environment on their photophysical properties. The intramolecular charge transfer in the molecule induces dipole moment. As photophysical properties are dependent on the extent of solute-solvent interaction and subsequently occurring intramolecular charge transfer phenomenon between donor and acceptor terminals. A prior knowledge of dipole moment of electronically excited short-lived species is of great importance in revelation of the nature of excited state, designing non linear optical material and parameterization of semi-empirical quantum chemical procedures of these states [28]. Among the techniques available for elucidation of the ground and excited state dipole moments, the most accepted technique is based on Lippert-Mataga equation [29–32]. This method is based on the shifts in the absorption and emission maxima with polarity functions of solvents, expressed by the relative permittivity (ε) and refractive index (η) of the solvent medium [33]. Hence solvatochromism and solvatofluorism are found to be excellent tools to evaluate the ground state and

Fig. 4 Emission spectra of dye
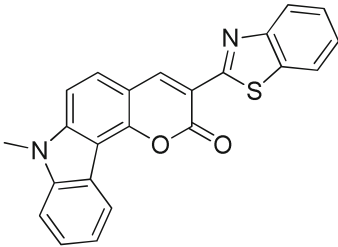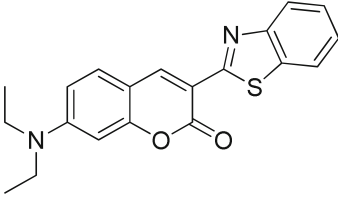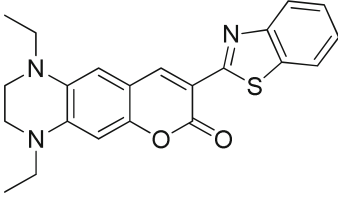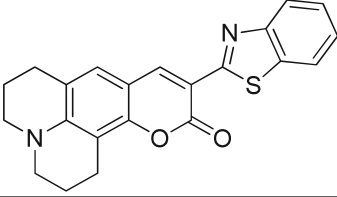**6a–6d** in different solvents
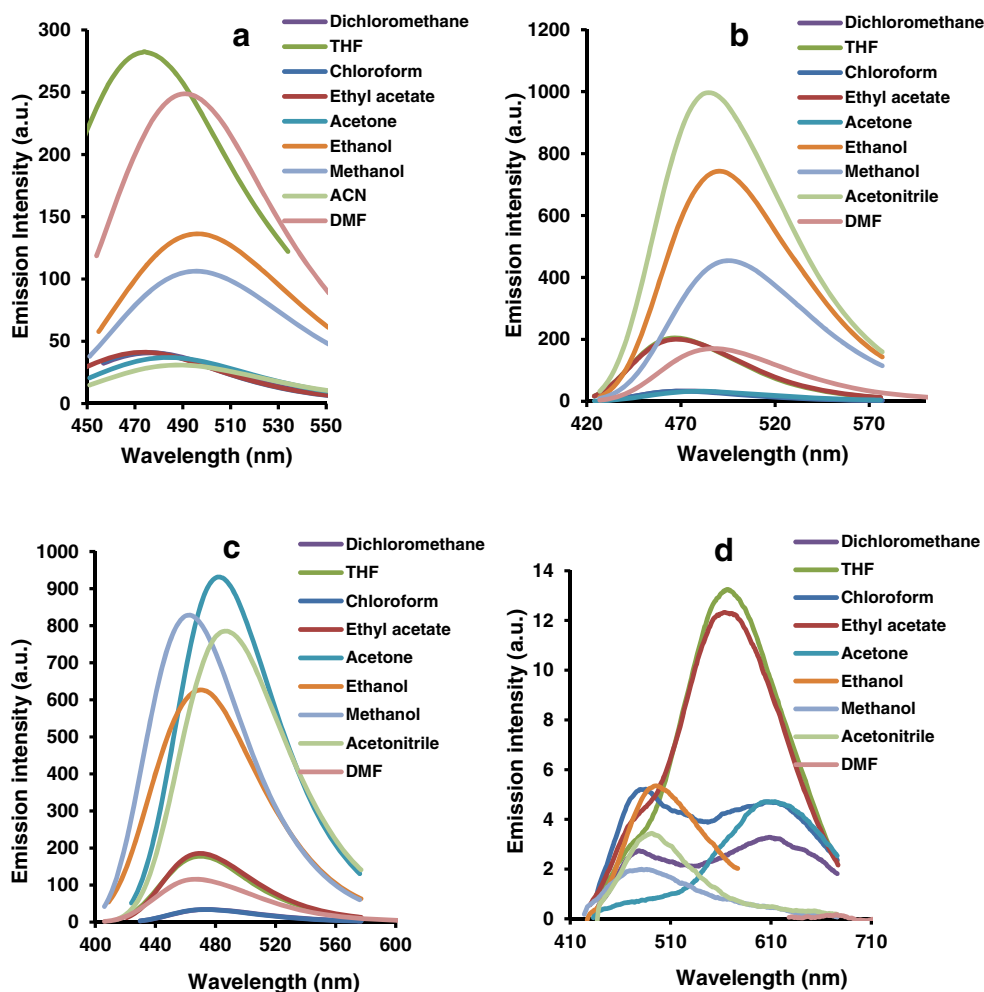
excited state dipole moments of the short-lived species [34–43].

The ratio of ground to excited state dipole moment of the synthesized novel coumarin dyes **6a–6d** calculated by using Bakhshiev [44] and Bilot-Kawski correlations [45–47]. It is to be noted that the formation of molecular complexes and hydrogen bonding does not accounted in the Lippert-Mataga relationship. It is to be noted that the formation of molecular complexes and hydrogen bonding does not account in the Lippert–Mataga relationship. A detailed theory for the calculation of dipole moment is described in supporting information [44, 45]. The calculated values of dipole moment in Table 2 demonstrate that the dyes **6c** and **6d** have highly polar excited state than the ground state, which accounts for the prominent charge transfer processes occurring in the excited state. While in the dyes **6a** and **6b** the ground state has higher dipole moment than the excited state indicating that the charge transfer processes occur in the ground state rather than in the excited state.

Computational Results

The different frontier molecular orbitals were studied to understand the electronic transition and charge delocalization within these donor-π-acceptor rigid chromophores. To gain further information about the structure orientation, electronic, photophysical and molecular properties of the compound we have performed theoretical calculations using density functional theory [B3LYP/6-31G(d)]. The angular twist of coumarin **6d** is shown in Fig. 5. The optimized structures for coumarins **6a-6d** are shown in Table 3. Frontier molecular orbital's of the dyes show that the LUMO of the compounds are invariably constituted by the chomone ring and electron acceptor unit like –CN, −NO$_2$, benzothiazoles and carboxylic acid group. HOMO is mainly on the N- methyl carbazole core. It is interesting to note that the HOMO of coumarin **6b** is spread over the carbazole and coumarin fragment but for other dyes it is mainly on carbazole core (Table 4). The comparative increase and decrease in the energy of the occupied (HOMO's) and virtual orbitals (LUMO's) gives a qualitative idea of the excitation properties and the ability of donor or

Table 1 Comparison of the spectral properties in CHCl$_3$ of the coumarin **6b** with related analogues

Coumarin	Structure	λ_{abs} (nm)	λ_{em} (nm)	$\Delta\lambda$ (nm)
Coumarin 6b		405	470	65
Coumarin 7		445	491	46
Coumarin 8		501	566	65
Coumarin 9		477	520	43

acceptor properties of the compounds. First allowed and the strongest electron transitions with largest oscillator strength usually correspond almost exclusively to the transfer of an electron from HOMO→LUMO (Tables 5, 6, 7, and 8) and shows the energies of different molecular orbitals involved in the electronic transitions of these coumarin dyes in different solvents. It is observed that the charge transfer band for all four dyes are mainly due to the electronic transition from highest occupied molecular orbital (HOMO) to lowest unoccupied molecular orbital (LUMO) whereas the other shorter electronic excitation is due to the HOMO-1→LUMO+1

Table 2 Excited state and ground state Dipole moment (in Debye) ratio value for coumarins **6a–6d**

Coumarin	$| m_1 + m_2 |$	$| m_1 - m_2 |$	$\dfrac{\mu_e}{\mu_g}$
6a	247.7	2237.6	0.11
6b	163.1	2519.7	0.06
6c	6242.4	3178.4	1.96
6d	9608.9	5160.4	1.86

transition for the coumarin **6a**. Noteworthy coumarins **6a–6d** showed a good correlation between the experimentally obtained absorption wavelength maxima and TD-B3LYP/6-31G(d) computed vertical excitation for these dyes (Table 9).

We have also performed theoretical calculation to calculate emission by TD-[B3LYP/6-31G(d)]. The experimental emissions of the coumarins **6a–6d** in the solvents of different polarities were compared with the emission obtained by TD-DFT computations (Table 9). The difference between the experimental emission and the computed emission is large in the polar solvents (methanol, ethanol, and DMF) as compared to the non-polar solvents (acetonitrile, DCM, chloroform, ethylacetate, acetone and THF).

The dipole moments of the coumarins **6a–6d** were computed in different solvents by DFT and TD-DFT (Table 10) to investigate the electronic behavior from the ground state (S$_0$) to the excited state (S$_1$) in different solvents. The dipole moments of the coumarins **6b–d** are more in the excited state as compared to the ground state; this is due to the fact that the excited state of the coumarins **6b–6d** is stabilized by salvation or hydrogen bonding with different solvents. In the case of the compound coumarin **6a**, the dipole moments are lower for the

Fig. 5 Angular twist in coumarin derivative **6d**
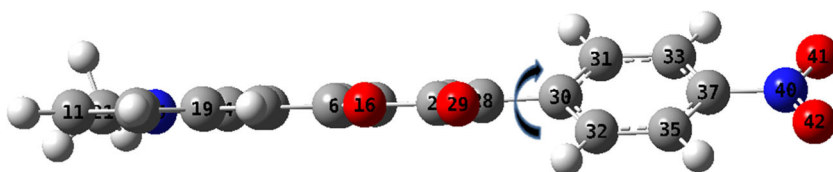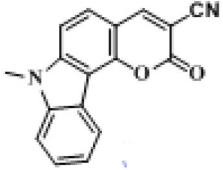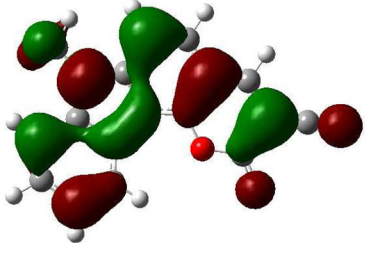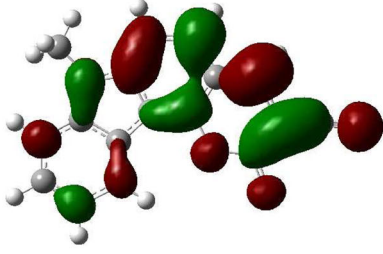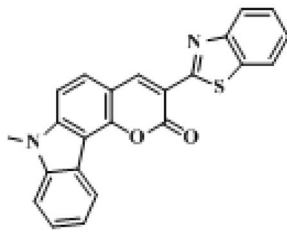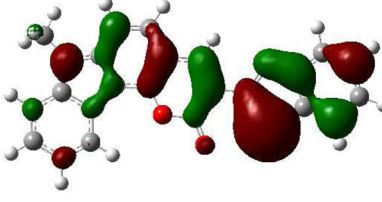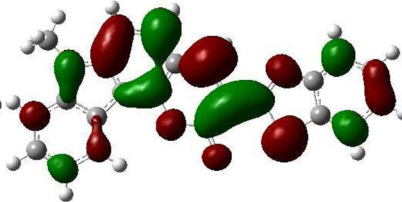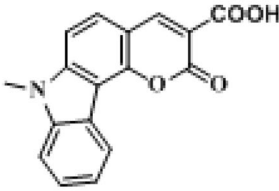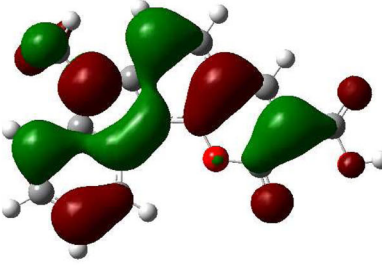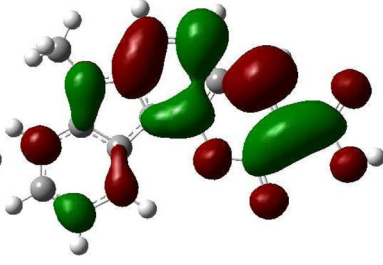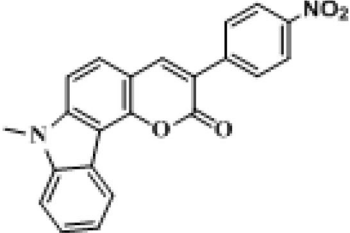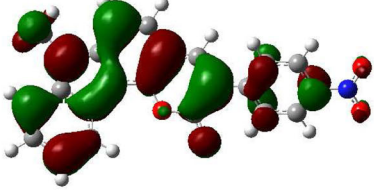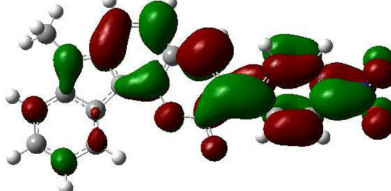

Table 3 Ground state optimized structures of coumarin 6a-d at B3LYP/6-31G(d) level of computation

Comp	Front view	Cross view
6a		
6b		
6c		
6d		

Table 4 Frontier molecular orbital's and its energy of coumarins **6a–d** in the ground and the excited state in acetonitrile solvent

Coumarin	HOMO	LUMO

excited state (S_1) and higher for the ground state (S_0); this is due to the fact that the ground state (S_0) of the coumarin **6a** is stabilized by the salvation or hydrogen bonding with the different solvents. The coumarin **6b** and **6c** shows a lower dipole moment as compared to the coumarins **6a** and **6d**. The trends in the dipole moment values reveal that the dipole moments of the coumarins **6a–6d** are higher in the polar solvents as compared to the non-polar solvents which can be attributed to the solvation effect.

Table 5 Observed UV-Visible absorption and computed absorption of coumarin **6a** in different solvents

Solvent	Experimental[a]	TD-B3LYP/6-31G(d)[b]		
	λ_{exct}^{max} (nm)	Vertical excitation (nm)	Oscillator strength, f (a.u.)	Major contribution[c]
MDC	407	394	0.3777	H→L (0.6614)
		270	0.4396	H-1→L +1 (0.6352)
THF	401	394	0.3730	H→L (0.6753)
		270	0.4366	H-1→L +1 (0.6347)
Chloroform	407	393	0.3854	H→L (0.6772)
		270	0.4483	H-1→L +1 (0.6369)
Ethyl acetate	398	393	0.3646	H→L (0.6737)
		270	0.4309	H-1→L +1 (0.6336)
Acetone	401	395	0.3585	H→L (0.6728)
		270	0.4220	H-1→L +1 (0.6317)
Ethanol	404	395	0.3590	H→L (0.6729)
		270	0.4220	H-1→L +1 (0.6317)
Methanol	401	395	0.3493	H→L (0.6711)
		270	0.4140	H-1→L +1 (0.6300)
Acetonitrile	404	395	0.3538	H→L (0.6720)
		270	0.4174	H-1→L +1 (0.6307)
DMF	404	396	0.3780	H→L (0.6763)
		270	0.4361	H-1→L +1 (0.6344)

[a] Experimental excitation wavelength λ_{exct}

[b] TD-B3LYP/6-31G(d) computations

[c] Electronic transitions (CI expansion coefficient for given transition); H=HOMO; L=LUMO

Experimental

Materials and Equipments

All the commercial reagents and solvents were procured from s. d. fine chemicals (India) and used as received without any further purification. The reaction was monitored by TLC using 0.25 mm E-Merck silica gel 60 F_{254} precoated plates, which were visualized with UV light. Melting points were measured on standard melting point apparatus from Sunder industrial product Mumbai, and are uncorrected. The FT-IR spectra were recorded on a Jasco- 4100 FT-IR Spectrometer. ^{1}H NMR spectra were recorded on Bruker 500 MHz and VXR 300 MHz instrument respectively using tetramethylsilane (TMS) as an internal standard. The visible absorption spectra of the compounds were recorded on a Spectronic Genesys 2 UV-Visible spectrophotometer. Fluorescence spectra of the compounds were recorded on Varian Cary eclipse spectrofluorimeter.

Computational Details

The ground state geometry of the compounds **6a–6d** (Table 3) in their Cs symmetry were optimized using the tight criteria in vacuum and in polar (DMF, ethanol, methanol, acetonitrile, and acetone) and non-polar (ethylacetate, chloroform, dichloromethane, and THF)

solvents using density functional theory [48] and Polarizable Continuum Model (PCM) [49, 50]. The functional used in this study was B3LYP. The B3LYP method combines Becke's three parameter exchange functional (B3) with the nonlocal correlation functional by Lee, Yang, and Parr (LYP)[51]. The basis set used for all atoms was 6-31G(d) the latter has been justified in the literature for the current investigation [52, 53]. The vertical excitation energies at the ground-state equilibrium geometries were calculated with TD-DFT [54–56]. The low-lying first singlet excited state (S1) of each tautomer was relaxed using the TD-DFT to obtain its minimum energy geometry. For computing the emissions the difference between the energies of the optimized geometries in the first singlet excited state and the ground state was used [57–59]. All electronic structure computations were carried out using the Gaussian 09 program [60].

Synthesis and Characterization

Synthesis of 4-Methoxy-9-Methyl-9H-Carbazole (**2**)

Sodium hydride 60 % (5.45 g, 136.45 mmol) was charged in 30 ml of dry THF and cooled to 0 °C under nitrogen atmosphere. 9H-Carbazole-4-ol (12.48 g, 68.22mmole) was added in 30 ml THF to it slowly maintaining

Table 6 Observed UV-Visible absorption and computed absorption of coumarin **6b** in different solvents

Solvent	Experimental[a]	TD-B3LYP/6-31G(d)[b]		
	λ_{exct}^{max} (nm)	Vertical excitation (nm)	Oscillator strength, f (a.u.)	Major contribution[c]
MDC	405	420	1.0163	H→L (0.7023)
		279	0.4080	H-1→L +1 (0.4975)
THF	399	420	1.0120	H→L (0.7022)
		279	0.4124	H-1→L +1 (0.5061)
Chloroform	405	419	1.0315	H→L (0.7024)
		279	0.4335	H-1→L +1 (0.5337)
Ethyl acetate	399	418	1.0035	H→L (0.7020)
		279	0.4154	H-1→L +1 (0.5166)
Acetone	399	420	0.9879	H→L (0.7018)
		280	0.3734	H-1→L +1 (0.4655)
Ethanol	402	420	0.9879	H→L (0.7018)
		280	0.3695	H-1→L +1 (0.4612)
Methanol	402	420	0.9748	H→L (0.7015)
		280	0.3602	H-1→L +1 (0.4548)
Acetonitrile	402	420	0.9804	H→L (0.7017)
		280	0.3609	H-1→L +1 (0.4540)
DMF	402	422	1.0105	H→L (0.7023)
		280	0.3716	H-1→L +1 (0.4568)

[a] Experimental excitation wavelength λ_{exct}
[b] TD-B3LYP/6-31G(d) computations
[c] Electronic transitions (CI expansion coefficient for given transition); H = HOMO; L = LUMO

temperature of reaction mass at 0 °C. Stirred for 30 min and then methyl iodide (8.70 ml, 136.45 mmol) was added. The reaction mass thus obtained brought to room temperature and stirred for 2 h under nitrogen atmosphere. Completion of the reaction was monitored by TLC. After completion of reaction, excess of sodium hydride is quenched by adding t-butyl alcohol under cooling conditions. Solvent was distilled out and added cold water to the residual mass stirred well and filtered. Crude 4-methoxy-9-methyl-9H-carbazole (**2**) obtained thus was purified by column chromatography on silica 60–120 mesh using toluene as eluent. Yield=93 %; Melting point=146–148 °C.

*Synthesis of 4-Methoxy-9-Methyl-9H-Carbazole Carbaldehyde (**3**)*

Phosphorous oxychloride (4.9 ml, 52.00 mmol) was added drop wise to DMF (17 ml, 219.53 mmol) at 0–5 °C, and stirred for 30 min maintaining the temperature 0–5 °C. 4-Methoxy-9-methyl-9H-carbazole 2 (10 g, 47.00 mmol) dissolved in 20 ml DMF was added drop wise within 30 min maintaining temperature between 0 and 5 °C. Stirring was continued for next 20–30 min, reaction mixture was then brought to room temperature and heated at 70–75° C for 1 h. Completion of the reation was monitored by TLC, shows formation of two major products. The obtained reaction mass poured into crushed ice stirred well and neutrilised with sodium bicarbonate.

Precipitate obtained was filtered off and dried. The crude product contains mixture of 4-methoxy-9-methyl-9H-carbazole-3-carbaldehyde (**3**) and 4-methoxy-9-methyl-9H-carbazole-1-carbaldehyde (**3a**). Separation of two individual compounds and purification was carried out by column chromatography on silica 100–200 mesh and using toluene as eluent.

Yield=48 %; Melting point=120–122 °C.
FT-IR (cm^{-1})=2844 (C-H aldehyde), 1662 (C=O), 1589 (C=C, aromatic).
^{1}H NMR (CDCl$_3$, 300 MHz)=δ 10.50 (s, 1H), 8.27 (d, 1H, J=8.4 Hz), 8.01 (d, 1H, J=8.4 Hz), 7.55 (t, 1H, J=7.7 & 7.3 Hz), 7.46 (d, 1H, J=7.7 Hz), 7.36 (t, 1H, J=8.0, 7.7 Hz) 7.25 (d, 1H, J=8.0 Hz), 4.19 (s, 3H), 3.90 (s, 3H).

*Synthesis of 4-Hydroxy-9-Methyl-9H-Carbazole-3-Carbaldehyde (**4**)*

4-Methoxy-9-methyl-9H-carbazole-3-carbaldehyde 3 (4 g, 16.74 mmol) dissolved in 20 ml of dry CH$_2$Cl$_2$ was added to a solution of AlCl$_3$ (8.8 g, 66 mmol) in 50 ml dry CH$_2$Cl$_2$ slowly in 30 min at 0 °C. The reaction mixture was further stirred at room temperature for 4 h. completion of reaction was monitored by TLC. The excess of AlCl$_3$ was neutralized with 0.1 N HCl stirred well and extracted with CH$_2$Cl$_2$ The solvent was evaporated and obtained residue was purified with column chromatography using toluene as eluent.

Table 7 Observed UV-Visible absorption and computed absorption of coumarin **6c** in different solvents

Solvent	Experimental[a]	TD-B3LYP/6-31G(d)[b]		
	λ_{exct}^{max} (nm)	Vertical excitation (nm)	Oscillator strength, f (a.u.)	Major contribution[c]
MDC	405	388	0.3837	H→L (0.6773)
		269	0.4748	H-1→L +1 (0.6394)
THF	396	387	0.3786	H→L (0.6764)
		269	0.4719	H-1→L +1 (0.6388)
Chloroform	405	386	0.3892	H→L (0.6777)
		269	0.4836	H-1→L +1 (0.6406)
Ethyl acetate	396	386	0.3697	H→L (0.6747)
		269	0.4664	H-1→L +1 (0.6378)
Acetone	399	388	0.3660	H→L (0.6746)
		269	0.4574	H-1→L +1 (0.6364)
Ethanol	384	389	0.3667	H→L (0.6748)
		269	0.4574	H-1→L +1 (0.6364)
Methanol	381	388	0.3574	H→L (0.6731)
		269	0.4496	H-1→L +1 (0.6350)
Acetonitrile	381	389	0.3619	H→L (0.6740)
		269	0.4529	H-1→L +1 (0.6356)
DMF	381	390	0.3855	H→L (0.6780)
		269	0.4712	H-1→L +1 (0.6389)

[a] Experimental excitation wavelength λ_{exct}
[b] TD-B3LYP/6-31G(d) computations
[c] Electronic transitions (CI expansion coefficient for given transition); H = HOMO; L = LUMO

Yield=67 %; Melting point=156–158 °C.
FT-IR (cm^{-1})=2834 (C-H aldehyde) 1739 (C=O), 1591 (C=C, aromatic).
Mass=m/z 226 (M+1).
^{1}H NMR (CDCl$_3$, 300 MHz)=9.88 (s, 1H), 8.38 (d, 1H, J=7.7 Hz), 7.55(d, 1H, J=8.4 Hz) 7.50 (t, 1H, J=7.7 & 8.4 Hz), 7.42 (d, 1H, J=8.0 Hz), 7.35 (t, 1H, J=7.7, 8.8 Hz), 7.00 (d, 1H, J=8.8 Hz), 4.77 (bs, 1H, OH), 3.87 (s, 3H).

Synthesis of 7-Methyl-2-Oxo-2,7-Dihydropyrano[3,2-c]Carbazole-3-Carbonitrile (6a)

4-Hydroxy-9-methyl-9*H*-carbazole-3-carbaldehyde (0.4 g, 1.8 mmol) and malononitrile (0.13 g, 2.0 mmol) was dissolved in 20 ml ethanol, catalytic amount of piperidine was added to it and refluxed for 2 h, bright yellow crystalline compound separate out. Completion of reaction was monitored by TLC. Reaction mass filtered and crude product obtained was purified by column chromatography using silica 100–200 mesh and toluene as eluent.

Yield=68 %; Melting point = >300 °C.
FT-IR (cm^{-1})=2221 (CN), 1724 (coumarin lactone).
Mass = m/z 275 (M+1).

^{1}H NMR (CDCl$_3$, 500 MHz) = δ 8.56 (d, 1H, J=7.5 Hz), 8.31(s, 1H), 7.61 (t, 1H, J=8, 7.5 Hz), 7.56 (d, 1H, J=8.5 Hz), 7.52 (d, 1H, J=8 Hz), 7.44 (t, 1H, J=7.5, 7.5 Hz), 7.40 (d, 1H, J=8.5 Hz), 3.97 (s, 3H).

Synthesis of 3-(Benzo[d]Thiazole-2-yl)-7-Methylpyrano[3,2-c]Carbazole-2(7H)-One (6b)

4-Hydroxy-9-methyl-9*H*-carbazole-3-carbaldehyde (0.4 g, 1.8 mmol) and 2-cyanomethyl-1,3-benzothiazole (0.34 g, 2.0 mmol) was stirred in 20 ml ethanol. Catalytic amount of piperidine was added to it and refluxed for 2 h, yellow product precipitate out. Completion of reaction was monitored by TLC. Yellow colored compound thus obtained was filtered and purified by column chromatography using silica 100–200 mesh and toluene as eluent.

Yield=84 %; Melting point=278–280 °C.
FT-IR (cm^{-1})=1701 (C=O), 1582 (C=C, aromatic).
Mass=m/z 383 (M+1).
^{1}H NMR (CDCl$_3$, 500 MHz)=δ 9.24 (s, 1H) 8.68 (d, 1H, J=7.3 Hz), 8.09 (d, 1H, J=8.4 Hz), 7.99 (d, 1H, J=9.1 Hz), 7.76 (d, 1H, J=8.8 Hz), 7.63-7.41 (m, 6H), 3.96 (s, 3H).

Table 8 Observed UV-Visible absorption and computed absorption of coumarin **6d** in different solvents

Solvent	Experimental[a] λ_{exct}^{max} (nm)	TD-B3LYP/6-31G(d)[b] Vertical excitation (nm)	Oscillator strength, f (a.u.)	Major contribution[c]
MDC	411	464	0.5432	H→L (0.7036)
		355	0.3218	H→L +1 (0.6891)
THF	411	463	0.5429	H→L (0.7036)
		355	0.3135	H→L +1 (0.6895)
		281	0.3074	H-2→L +1 (0.4788)
Chloroform	411	458	0.5674	H→L (0.7033)
		353	0.2937	H→L +1 (0.6908)
		280	0.2297	H-2→L +1 (0.5774)
Ethyl acetate	405	460	0.5418	H→L (0.7036)
		354	0.3016	H→L +1 (0.6899)
		280	0.2657	H-2→L +1 (0.5390)
Acetone	408	468	0.5147	H→L (0.7040)
		356	0.3374	H→L +1 (0.6873)
Ethanol	402	469	0.5134	H→L (0.7040)
		356	0.3406	H→L +1 (0.6871)
Methanol	399	469	0.5036	H→L (0.7041)
		356	0.3411	H→L +1 (0.6866)
Acetonitrile	411	470	0.5067	H→L (0.7041)
		357	0.3433	H→L +1 (0.6866)
DMF	417	471	0.5257	H→L (0.7039)
	603	357	0.3503	H→L +1 (0.68692)

[a] Experimental excitation wavelength λ_{exct}

[b] TD-B3LYP/6-31G(d) computations

[c] Electronic transitions (CI expansion coefficient for given transition); H = HOMO; L = LUMO

Synthesis of 7-Methyl-2-Oxo-2,7-Dihydropyrano[3,2-c] Carbazole-3-Carboxylic Acid (6c)

4-Hydroxy-9-methyl-9*H*-carbazole-3-carbaldehyde (0.4 g, 1.8 mmol) and Meldrum's acid (0.26 g, 1.8 mmol) was stirred in 20 ml ethanol. Catalytic amount of piperidine was added to it and heated to reflux for 2 h, bright yellow crystal separate out. Completion of the reaction was monitored by TLC. Filtered the reaction mass and crud product obtained was purified by recrystallization in methanol solvent.

Table 9 Observed and computed emission of coumarin **6a–6d**

Solvents	6a λ_{ems}^{max} (nm) Exp.[a]	TD-B3LYP/ 6-31G(d) emission (nm)[b]	6b λ_{ems}^{max} (nm) Exp.[a]	TD-B3LYP/ 6-31G(d) emission (nm)[b]	6c λ_{ems}^{max} (nm) Exp.[a]	TD-B3LYP/ 6-31G(d) emission (nm)[b]	6d λ_{ems}^{max} (nm) Exp.[a]	TD-B3LYP/ 6-31G(d) emission (nm)[b]
Dichloromethane	477	436	473	459	476	427	479	505
THF	474	435	467	457	470	427	566	502
Chloroform	475	432	470	452	473	424	485	494
Ethyl acetate	474	434	468	455	469	425	564	499
Acetone	484	438	480	463	482	430	613	514
Ethanol	496	438	491	464	470	430	495	515
Methanol	496	439	496	465	463	431	481	517
Acetonitrile	488	439	485	465	486	431	491	518
DMF	491	439	488	465	466	431	503	517

[a] Experimentally recorded emission maxima

[b] Emission computed using TD-B3LYP/6-31G(d) level

Table 10 The dipole moments of the coumarins **6a–d** were computed in different solvents by DFT and TD-DFT

Solvent medium	6a		6b		6c		6d	
	μg	μe	μg	μe	μg	μe	μ_g	μe
Dichloromethane	14.4	14.2	9.3	10.2	9.7	9.9	14.3	15.0
THF	14.3	14.0	9.2	10.0	9.6	9.8	14.2	14.8
Chloroform	13.8	13.8	8.8	9.6	9.3	9.4	13.8	14.1
Ethyl acetate	14.1	14.8	9.0	9.9	9.5	9.6	14.0	14.5
Acetone	14.9	14.6	9.6	10.6	10.1	10.3	14.7	15.5
Ethanol	14.9	14.7	9.6	10.6	10.1	10.4	14.8	15.6
Methanol	15.0	14.8	9.7	10.7	10.2	10.5	14.8	15.7
Acetonitrile	15.0	14.8	9.7	10.7	10.2	10.5	14.8	15.8
DMF	15.0	14.8	9.7	10.7	10.2	10.5	14.9	15.8

Yield=81 %; Melting point=271 °C (decomposes).
FT-IR (cm^{-1})=1742 (C=O), 1584 (C=C, aromatic).
Mass=m/z 294 (M+1).
^{1}H NMR (CDCl$_3$, 500 MHz)=δ 12.92 (bs, 1H), 8.92 (s, 1H), 8.35 (d, 1H, J=7.5 Hz), 7.95 (d, 1H, J=8.5 Hz), 7.77 (d, 1H, J=8 Hz), 7.71 (d, 1H, J=8.5 Hz), 7.61 (t, 1H, J=7, 8 Hz), 7.43 (t, 1H, J=8,7 Hz), 4.00 (s, 3H).

*Synthesis of 7-Methyl-3-(4-Nitrophenyl)Pyrano[3,2-c] Carbazole-2(7H)-One (**6d**)*

4-Hydroxy-9-methyl-9*H*-carbazole-3-carbaldehyde (0.4 g, 1.8 mmol) and p-nitrobenzyl cyanide (0.29 g, 1.8 mmol) was dissolved in ethanol. To this solution catalytic amount of piperidine was added and refluxed for 2 h to give dark yellow product. Completion of reaction was monitored by TLC. Filtered the reaction mass and crud product obtained was purified by column chromatography using 100–200 mesh silica and toluene as eluent.

Yield=81 %; Melting point=290–292 °C.
FT-IR (cm^{-1})=1650 (C=O), 1586 (C=C, aromatic).
Mass=m/z 370 (M+1).
^{1}H NMR (CDCl$_3$, 500 MHz)=δ 9.00 (s, 1H), 8.63 (d, 1H, J=7 Hz), 8.29 (d, 2H, J=8.5 Hz), 8.14 (d, 1H, J=7 Hz), 7.70–7.65 (m, 2H), 7.56 (t, 1H, J=7.5, 7 Hz), 7.49 (d, 2H, J=8.5 Hz), 7.34 (t, 1H, J=7.5, 7.5 Hz), 3.95 (s, 3H).

Conclusion

In conclusion, we have successfully synthesized novel coumarin analogues **6a–6d** with a rigid donor N-methyl-4-hydroxy carbazole. These coumarin derivatives are highly fluorescent and emits in the blue region. Coumarin dyes **6a–6c** absorb in the region 463 to 496 nm, while **6d** shows dual absorption in DMF and dual emission in chloroform, dichloromethane and chloroform, it has largest Stokes' shift of 205 nm in acetone. These properties observed in **6d** are due to intramolecular charge transfer induced by solute-solvent interaction. All these synthesized coumarin derivatives are sensitive towards solvent polarity and shows good to excellent solvatochromism and solvatofluorism characteristics. Dipole moment calculations show that in case of dyes **6a** and **6b** ground state is more polarized than the excited state. While in dyes **6c** and **6d** excited state is more polarized than the ground state.

References

1. Li H, Cai L, Chen Z (2012) Coumarin-derived fluorescent chemosensors. In: Wang W (ed) Adv Chem Sensors pp 121–150
2. Drexhage KH (1973) Dye lasers. Topics in applied physics
3. Krasovitskii BM (1988) Organic luminescent materials. Wiley-VCH Weinheim, Germany
4. Nourmohammadian F, Gholami MD (2010) Microwave-promoted one-pot syntheses of coumarin dyes. Synth Commun 40:901–909
5. Essaïdi Z, Krupka O, Iliopoulos K et al (2013) Synthesis and functionalization of coumarin-containing copolymers for second order optical nonlinearities. Opt Mater (Amst) 35:576–581
6. Maity D, Karthigeyan D, Kundu TK, Govindaraju T (2013) FRET-based rational strategy for ratiometric detection of Cu2+ and live cell imaging. Sensors Actuators B Chem 176:831–837
7. Ye D, Wang L, Li H et al (2013) Synthesis of coumarin-containing conjugated polymer for naked-eye detection of DNA and cellular imaging. Sensors Actuators B Chem 181:234–243
8. Signore G, Nifosì R, Albertazzi L et al (2010) Polarity-sensitive coumarins tailored to live cell imaging. J Am Chem Soc 132:1276–1288
9. Wang T, Zhao Y, Shi M, Wu F (2007) The synthesis of novel coumarin dyes and the study of their photoreaction properties. Dye Pigment 75:104–110

10. Corrie JET, Munasinghe VRN, Rettig W (2000) Synthesis and fluorescence properties of substituted 7-aminocoumarin-3-carboxylate derivatives. J Heterocycl Chem 37:1447–1455

11. Lin Q, Bao C, Fan G et al (2012) 7-amino coumarin based fluorescent phototriggers coupled with nano/bio-conjugated bonds: synthesis, labeling and photorelease. J Mater Chem 22:6680–6688

12. Grandberg II, Denisov LK, Popova OA (1987) 7-aminocoumarins (Review). Chem Heterocycl Compd 23:117–142

13. Reddy AR, Prasad DV, Darbarwar M (1986) Absorption and fluorescence spectra of 7-aminocoumarin derivatives. J Photochem 32:69–80

14. Kim E, Park SB (2010) In: Demchenko AP (ed) Advanced fluorescence reporters in chemistry and biology I: fundamentals and biology, fundamentals and molecular design. Springer, Heidelberg, pp 150–155

15. Jagtap AR, Satam VS, Rajule RN, Kanetkar VR (2009) The synthesis and characterization of novel coumarin dyes derived from 1,4-diethyl-1,2,3,4-tetrahydro-7-hydroxyquinoxalin-6-carboxaldehyde. Dye Pigment 82:84–89

16. Besson T, Coudert G, Guillaumet G (1991) Synthesis and fluorescent properties of some heterobifunctional and rigidized 7-aminocoumarins. J Heterocycl Chem 28:1517–1523

17. Reynolds GA, Drexhage KH (1975) New coumarin dyes with rigidized structure for flashlamp-pumped dye lasers. Opt Commun 13:222–225

18. Abdel-Mottaleb MSA, Antonious MS, Abo-Aly MM et al (1989) Photophysics and dynamics of rigidized coumarin laser dyes. J Photochem Photobiol A Chem 50:259–273

19. Wada T, Zhang Y, Choi YS, Sasabe H (1993) Photoconductive crystals for nonlinear optics: molecular design and crystal structure. J Phys D Appl Phys 26:B221

20. Wada T, Zhang Y, Yamakado M, Sasabe H (1993) Linear and nonlinear optical properties of carbazole-containing polymers. Mol Cryst Liq Cryst Sci Technol Sect A Mol Cryst Liq Cryst 227:85–92

21. Chang C-C, Kuo I-C, Lin J-J et al (2004) A novel carbazole derivative, BMVC: a potential antitumor agent and fluorescence marker of cancer cells. Chem Biodivers 1:1377–1384

22. Qian Y, Xiao G, Wang G et al (2006) Synthesis and third-order optical nonlinearity in two-dimensional A-π-D-π-A carbazole-cored chromophores. Dye Pigment 71:109–117

23. Fitilis I, Fakis M, Polyzos I et al (2007) A two-photon absorption study of fluorene and carbazole derivatives. The role of the central core and the solvent polarity. Chem Phys Lett 447:300–304

24. Li H, Zhang Y, Hu Y et al (2004) Novel soluble N-phenyl-carbazole-containing PPVs for light-emitting devices: synthesis, electrochemical, optical, and electroluminescent properties. Macromol Chem Phys 205:247–255

25. Thomas KRJ, Lin JT, Tao Y-T, Ko C-W (2000) Novel green light-emitting carbazole derivatives: potential electroluminescent materials. Adv Mater 12:1949–1951

26. Kuo W-J, Hsiue G-H, Jeng R-J (2002) Synthesis and macroscopic second-order nonlinear optical properties of poly(ether imide)s containing a novel two-dimensional carbazole chromophore with nitro acceptors. J Mater Chem 12:868–878

27. Zhou Y, Wang F, Kim Y et al (2009) Cu2+−selective ratiometric and "off-on" sensor based on the rhodamine derivative bearing pyrene group. Org Lett 11:4442–4445

28. Ravi M, Samanta A, Radhakrishnan TP (1994) Excited state dipole moments from an efficient analysis of solvatochromic stokes shift data. J Phys Chem 98:9133–9136

29. Lippert E (1957) Spektroskopische bestimmung des dipolmomentes aromatischer verbindungen im ersten angeregten singulettzustand. Zeitschrift für Elektrochem Ber Bunsenges Phys Chem 61:962–975

30. Mataga N, Kaifu Y, Koizumi M (1955) The solvent effect on fluorescence spectrum, change of solute-solvent interaction during the lifetime of excited solute molecule. Bull Chem Soc Jpn 28:690–691

31. Mataga N (1963) Solvent effects on the absorption and fluorescence spectra of naphthylamines and isomeric aminobenzoic acids. Bull Chem Soc Jpn 36:654–662

32. Mataga N, Kaifu Y, Koizumi M (1956) Solvent effects upon fluorescence spectra and the dipolemoments of excited molecules. Bull Chem Soc Jpn 29:465–470

33. Reichardt C (2002) Solvents and solvent effects in organic chemistry

34. Ravi M, Soujanya T, Samanta A, Radhakrishnan TP (1995) Excited-state dipole moments of some coumarin dyes from a solvatochromic method using the solvent polarity parameter, E N T. J Chem Soc Faraday Trans 91:2739

35. Kumar S, Rao VC, Rastogi RC (2001) Excited-state dipole moments of some hydroxycoumarin dyes using an efficient solvatochromic method based on the solvent polarity parameter, ETN. Spectrochim Acta Part A Mol Biomol Spectrosc 57:41–47

36. Masternak A, Wenska G, Milecki J et al (2005) Solvatochromism of a novel Betaine dye derived from purine. J Phys Chem A 109:759–766

37. Nemkovich NA, Pivovarnko VG, Baumann W et al (2005) Dipole moments of 4 -aminoflavonol fluorescent probes in different solvents. J Fluoresc 15:29–36

38. Aaron J-J, Maafi M, Kersebet C et al (1996) A solvatochromic study of new benzo[a]phenothiazines for the determination of dipole moments and specific solute—solvent interactions in the first excited singlet state. J Photochem Photobiol A Chem 101:127–136

39. Raikar US, Renuka CG, Nadaf YF et al (2006) Rotational diffusion and solvatochromic correlation of coumarin 6 laser dye. J Fluoresc 16:847–854

40. Inamdar SR, Nadaf YF, Mulimani BG (2003) Ground and excited state dipole moments of exalite 404 and exalite 417 UV laser dyes determined from solvatochromic shifts of absorption and fluorescence spectra. J Mol Struct THEOCHEM 624:47–51

41. Harbison GS (2002) The electric dipole polarity of the ground and low-lying metastable excited states of NF. J Am Chem Soc 124:366–367

42. Hodge CN, Aldrich PE, Wasserman ZR et al (1999) Corticotropin-releasing hormone receptor antagonists: framework design and synthesis guided by ligand conformational studies. J Med Chem 42:819–832

43. Józefowicz M, Heldt JR (2007) Dipole moments studies of fluorenone and 4-hydroxyfluorenone. Spectrochim Acta Part A Mol Biomol Spectrosc 67:316–320

44. Bakhshiev NG (1964) Opt Spektrosk 16:821–832

45. Kawski A (1966) Zur lösungsmittelabhängigkeit der wellenzahl von elektronenbanden lumineszierender moleküle und über die bestimmung der elektrischen dipolmomente im anregungszustand. Acta Phys Polon 29:507–518

46. Chamma A, Viallet PCR (1970) Determination du moment dipolaire d'une molecule dans un etat excite singulet. Acad Sci Paris Ser C 270:1901–1904

47. Kawski A (1964) Dipolmomente einiger Naphthole im Grund- und Anregungszustand. Naturwissenschaften 51:82–83

48. Treutler O, Ahlrichs R (1995) Efficient molecular numerical integration schemes. J Chem Phys 102:346–354

49. Cossi M, Barone V, Cammi R, Tomasi J (1996) Ab initio study of solvated molecules: a new implementation of the polarizable continuum model. Chem Phys Lett 255:327–335

50. Tomasi J, Mennucci B, Cammi R (2005) Quantum mechanical continuum solvation models. Chem Rev 105:2999–3094

51. Lee C, Yang W, Parr RG (1988) Development of the Colle-Salvetti correlation-energy formula into a functional of the electron density. Phys Rev B 37:785–789

52. Kim CH, Park J, Seo J et al (2010) Excited state intramolecular proton transfer and charge transfer dynamics of a 2-(2′-hydroxyphenyl)benzoxazole derivative in solution. J Phys Chem A 114:5618–5629

53. Casida ME, Jamorski C, Casida KC, Salahub DR (1998) Molecular excitation energies to high-lying bound states from time-dependent density-functional response theory: characterization and correction of

the time-dependent local density approximation ionization threshold. J Chem Phys 108:4439–4449

54. Furche F, Rappaport D (2005) Density functional theory for excited states: equilibrium structure and electronic spectra. In: Computational photochemistry

55. Hehre WJ, Radom L, Schleyer PV, Pople J (1986) Ab initio molecular orbital theory. Wiley, New York

56. Bauernschmitt R, Ahlrichs R (1996) Treatment of electronic excitations within the adiabatic approximation of time dependent density functional theory. Chem Phys Lett 256:454–464

57. Lakowicz JR (1999) Principles of fluorescence spectroscopy, 2nd edn. New York, Kluwer Academic

58. Phatangare KR, Gupta VD, Tathe AB et al (2013) ESIPT inspired fluorescent 2-(4-benzo[d]oxazol-2-yl)naphtho[1,2-d]oxazol-2-yl)phenol: experimental and DFT based approach to photophysical properties. Tetrahedron 69:1767–1777

59. Valeur B, Berberan-Santos MN (2001) Molecular fluorescence: principles and applications. Weinheim, Wiley-VCH Verlag

60. Frisch MJ, Trucks GW, Schlegel HB et al (2009) Gaussian 09, Revision C.01. Gaussian 09, Revis B.01. Gaussian, Inc, Wallingford